

# Multimodal mechanisms of human socially reinforced learning across neurodegenerative diseases

Agustina Legaz,<sup>1,2,3</sup> Sofia Abrevaya,<sup>2,4</sup> Martín Dottori,<sup>1</sup> Cecilia González Campo,<sup>1,2</sup> Agustina Birba,<sup>1,2</sup> Miguel Martorell Caro,<sup>2,4</sup> Julieta Aguirre,<sup>5</sup> Andrea Slachevsky,<sup>6,7,8,9</sup> Rafael Aranguiz,<sup>10</sup> Cecilia Serrano,<sup>11</sup> Claire M. Gillan,<sup>12,13,14</sup> Iracema Leroi,<sup>12</sup> Adolfo M. García,<sup>1,2,12,15,16,17</sup> Sol Fittipaldi,<sup>1,2,3</sup> and Agustín Ibañez<sup>1,2,12,18</sup>

## Abstract

Social feedback can selectively enhance learning in diverse domains. Relevant neurocognitive mechanisms have been studied mainly in healthy persons, yielding correlational findings. Neurodegenerative lesion models, coupled with multimodal brain measures, can complement standard approaches by revealing direct multidimensional correlates of the phenomenon. To this end, we assessed socially reinforced and non-socially reinforced learning in 40 healthy participants as well as persons with behavioral variant frontotemporal dementia ( $n = 21$ ), Parkinson's disease ( $n = 31$ ), and Alzheimer's disease ( $n = 20$ ). These conditions are typified by predominant deficits in social cognition, feedback-based learning, and associative learning respectively, although all three domains may be partly compromised in the other conditions. We combined a validated behavioral task with ongoing electroencephalographic (EEG) signatures of implicit learning (medial frontal negativity) and offline magnetic resonance imaging (MRI) measures (voxel-based morphometry). In healthy participants, learning was facilitated by social feedback relative to non-social feedback. In comparison with controls, this effect was specifically impaired in behavioral variant frontotemporal dementia and Parkinson's disease, while unspecific learning deficits (across social and non-social conditions) were observed in Alzheimer's disease. EEG results showed increased medial frontal negativity in healthy controls during social feedback and learning. Such a modulation was selectively disrupted in behavioral variant frontotemporal dementia. Neuroanatomical results revealed extended temporo-parietal and fronto-limbic correlates of socially reinforced learning, with specific temporo-parietal associations in behavioral variant frontotemporal dementia, and predominantly fronto-limbic regions in Alzheimer's disease. In contrast, non-socially reinforced learning was consistently linked to medial temporal/hippocampal regions. No associations with cortical volume were found in Parkinson's disease. Results are consistent

© The Author(s) (2021). Published by Oxford University Press on behalf of the Guarantors of Brain.

This is an Open Access article distributed under the terms of the Creative Commons Attribution Non-Commercial License (<http://creativecommons.org/licenses/by-nc/4.0/>), which permits non-commercial re-use, distribution, and reproduction in any medium, provided the original work is properly cited. For commercial re-use, please contact [journals.permissions@oup.com](mailto:journals.permissions@oup.com)

with core social deficits in behavioral variant frontotemporal dementia, subtle disruptions in ongoing feedback-mechanisms and social processes in Parkinson's disease, and generalized learning alterations in Alzheimer's disease. This multimodal approach highlights the impact of different neurodegenerative profiles on learning and social feedback. Our findings inform a promising theoretical and clinical agenda in the fields of social learning, socially-reinforced learning and neurodegeneration.

**Author affiliations:**

1 Cognitive Neuroscience Center (CNC), Universidad de San Andrés, Buenos Aires, C1011ACC, Argentina

2 National Scientific and Technical Research Council (CONICET), Buenos Aires, C1425FQB, Argentina

3 Universidad Nacional de Córdoba. Facultad de Psicología, Córdoba, CU320, Argentina

4 Institute of Cognitive and Translational Neuroscience (INCYT), INECO Foundation, Favaloro University, CONICET, Buenos Aires, C1021, Argentina

5 Instituto de Investigaciones Psicológicas (IIPsi), CONICET, Universidad Nacional de Córdoba, Córdoba, CB5000, Argentina

6 Memory and Neuropsychiatric Clinic (CMYN) Neurology Department, Hospital del Salvador, SSMO & Faculty of Medicine, University of Chile, Santiago, Chile

7 Gerosciences Center for Brain Health and Metabolism, Santiago, Chile

8 Neuropsychology and Clinical Neuroscience Laboratory, Physiopathology Department, ICBM, Neurosciences Department, Faculty of Medicine, University of Chile, Chile

9 Servicio de Neurología, Departamento de Medicina, Clínica Alemana-Universidad del Desarrollo, Chile

10 Instituto Nacional de Geriatria, Santiago, Chile

11 Neurología Cognitiva, Hospital Cesar Milstein, Buenos Aires, C1221, Argentina

12 Global Brain Health Institute (GBHI), University of California San Francisco (UCSF), San Francisco, CA 94158, USA

13 Department of Psychology, Trinity College Dublin, Dublin, Ireland

14 Trinity College Institute of Neuroscience, Trinity College Dublin, Dublin, Ireland

15 Global Brain Health Institute (GBHI), Trinity College Dublin (TCD), Dublin, Dublin 2, Ireland

16 Faculty of Education, National University of Cuyo, Mendoza, M5502JMA, Argentina

17 Departamento de Lingüística y Literatura, Facultad de Humanidades, Universidad de Santiago de Chile, Santiago, Chile

18 Latin American Brain Health Institute (BrainLat), Universidad Adolfo Ibáñez, Santiago, Chile

Correspondence to: Sol Fittipaldi

Centro de Neurociencias Cognitivas (CNC) and CONICET; Vito Dumas 284, B1644BID Victoria, Buenos Aires, Argentina

E-mail: [fittipaldisol@gmail.com](mailto:fittipaldisol@gmail.com)

Correspondence may also be addressed to: Agustín Ibáñez

E-mail: [agustin.ibanez@gbhi.org](mailto:agustin.ibanez@gbhi.org)

**Running title:** Social learning in neurodegeneration

**Keywords:** learning; social reinforcement; behavioral variant frontotemporal dementia; Alzheimer's disease; Parkinson's disease

**Abbreviations:** AD = Alzheimer's disease; BvFTD = behavioral variant frontotemporal dementia; HCs = healthy controls; GM = grey matter; MFN = medial frontal negativity; NINCDS-ADRDA = National Institute of Neurological and Communicative Disorders and Stroke - Alzheimer's Disease and Related Disorders Association; NSRL = non-socially reinforced learning; PD = Parkinson's disease; SPM12 = Statistical Parametric Mapping

software v.12; SnPM = statistical non-parametric mapping; SRL = socially reinforced learning; VBM = voxel-based morphometry

## Introduction

Social reinforcement is a powerful facilitator of learning,<sup>1-4</sup> especially relative to non-social feedback.<sup>5-10</sup> Contextual interpersonal cues like facial emotional expressions<sup>11, 12</sup> promote associative learning<sup>10, 13</sup> by engaging emotional arousal and reward/punishment mechanisms.<sup>14-16</sup> According to the social-context network model, these integrative processes implicate a broad fronto-insulo-temporal network,<sup>17-22</sup> with socially reinforced learning (SRL) depending critically on temporo-parietal hubs, and secondarily on fronto-limbic hubs, both related to context-target associative learning and social cognition.<sup>20, 21, 23-27</sup> However, most evidence comes from healthy individuals, offering limited (correlational) information to identify critical neural signatures. The neurodegenerative lesion model approach partially overcomes these limitations by revealing direct links between affected brain mechanisms and behavioral performance.<sup>28-32</sup> Yet, while some works have examined social vs. non-social learning in neurodegenerative diseases<sup>33, 34</sup> (**Table 1**), and others have addressed SRL through neurophysiological methods,<sup>25, 26, 35</sup> no study has integrated both approaches – let alone with a multimodal framework. Here, we examined behavioral, electroencephalographic (EEG) and structural neuroimaging correlates of a SRL paradigm in healthy controls (HCs) as well as people with behavioral variant frontotemporal dementia (bvFTD), Parkinson's disease (PD), and Alzheimer's disease (AD), typified by predominant deficits in social cognition, feedback-based learning, and associative learning, respectively.

Preliminary psychophysiological evidence (behavioral and EEG studies) points to different patterns of disturbance across neurodegenerative subtypes. In bvFTD, impaired processing of socially relevant information<sup>36, 37</sup> is particularly evident in associative learning tasks.<sup>33, 36</sup> Such deficits have been linked to disruptions of social reward processing<sup>36, 38</sup> and contextual integration skills.<sup>18, 39, 40</sup> In PD, although impaired feedback-based learning has been reported,<sup>41-43</sup> no study has compared performance in social and non-social feedback conditions, despite reported socioemotional disturbances in this disease.<sup>44-46</sup> In AD, although

socioemotional functions usually remain partially intact in mild-moderate stages,<sup>47, 48</sup> facial cues do not enhance associative learning<sup>33, 36</sup> – but see.<sup>34</sup> Altogether, beyond reported overlapping disruptions in memory and social cognition domains across neurodegenerative conditions,<sup>47, 49-51</sup> behavioral evidence points to predominately socio-contextual learning impairments in bvFTD, implicit learning and socioemotional disturbances in PD, and general learning deficits in AD. Finally, EEG evidence of SRL is limited in neurodegenerative conditions. While social processing impairments have been related to diminished frontal EEG activity in bvFTD,<sup>40</sup> no previous work has associated SRL with ongoing EEG activity in other neurodegenerative diseases.

Neuroimaging evidence of SRL is also scant. In bvFTD, social learning impairments have been related to orbitofrontal and temporal grey matter (GM) atrophy.<sup>36</sup> With regards to PD, although a link between feedback-based learning impairments and cortico-striatal dysfunctions has been assumed,<sup>41, 43</sup> no previous work has directly examined structural associations with SRL in this group. Finally, in AD, disrupted social enhancement in associative learning has been related to medial temporal and parietal atrophy.<sup>6, 36, 52</sup>

Although social and feedback-based learning have been separately assessed in in bvFTD, PD and AD (**Table 1**), no previous work has jointly addressed SRL in neurodegenerative models that differentially impact social cognition, feedback-based learning, and general associative learning. To our knowledge, this is the first feedback-based associative learning study combining social and non-social cues in neurodegeneration. Moreover, no previous work has targeted SRL/NSRL while tracking ongoing EEG correlates in different neurodegenerative groups- let alone in a multidimensional approach combining behavioral, EEG and neuroimaging.

Our approach enables the joint assessment of feedback-related mechanisms across behavioral, neurophysiological, and neuroanatomical dimensions. We adapted an associative learning paradigm, previously reported with healthy participants,<sup>10</sup> that evaluates how social and non-social feedback impacts implicit learning of an arbitrary association between two stimulus types. Specifically, the task requires participants to judge the category membership ('A' or 'B') of repeatedly presented three-digit numbers, and learn (across different cycles) the correct association upon receiving feedback via socioemotional facial expressions (SRL) or colored circles (NSRL) after each number-category judgment. Learning is indexed by increased

accuracy and/or response time across cycles. High-density EEG allowed tracking ongoing markers of feedback-based learning via medial frontal negativity (MFN) modulations,<sup>53-55</sup> a group of event-related potentials (error-related negativity, feedback-related negativity, and N2) sensitive to cognitive demands and strategic on-the-fly adjustments.<sup>54, 55</sup> Specifically, larger MFN is predictive of enhanced learning by feedback<sup>53, 56, 57</sup> Moreover, magnetic resonance imaging (MRI) recordings were obtained offline to investigate neuroanatomical correlates of SRL.

In HCs, we predicted enhanced performance across the task (final > initial trials), with better performance after social relative to non-social feedback (SRL > NSRL).<sup>10, 13</sup> Similarly, we expected that both effects would be associated with larger MFN.<sup>53, 56-58</sup> Also, in line with the social-context network model, we predicted that SRL performance would be related with extended temporo-posterior (and, to a lesser degree, frontal) regions involved in socio-contextual processing and learning.<sup>20, 21, 24, 25</sup> Conversely, we anticipated that NSRL would be associated with regions underpinning associative learning (i.e., hippocampal and medial temporal lobe structures).<sup>6, 59</sup>

Furthermore, in comparison with controls, distinct SRL disruptions were predicted for each neurodegenerative group. In bvFTD, due to its well-known social processing impairments, we expected reduced social-feedback facilitation on behavioral performance, alongside diminished MFN modulations for SRL relative to NSRL, as well as brain-behavior associations across temporo-posterior regions in (impaired) SRL and hippocampal regions in (preserved) NSRL. In PD, considering prominent feedback-related learning and socioemotional disturbances, we predicted behavioral SRL deficits and impaired MFN modulations during final trials. Regarding AD, we hypothesized behavioral impairments in both feedback conditions (SRL and NSRL), along with diminished MFN modulations during final trials (in contrast to HCs), resembling generalized learning deficits, associated with temporo-posterior atrophy. By jointly testing these hypotheses, we aim to provide convergent multimodal evidence of SRL disruptions across neurodegenerative diseases.

## Materials and methods

## Participants

The study comprised 112 participants: 40 HCs with preserved cognition and no history of neuropsychiatric diseases and/or substance abuse; 21 people fulfilling revised criteria for bvFTD<sup>60</sup>; 31 people with PD diagnosed in accordance with the United Kingdom PD Society Brain Bank criteria<sup>61</sup>; and 20 people with AD, each fulfilling the international NINCDS-ADRDA criteria.<sup>62, 63</sup> Power analyses confirmed the adequacy of our sample size (**Supplementary Material 1.1**). Participants were recruited from three international clinics taking part in the Multi-Partner Consortium to Expand Dementia Research in Latin America (ReDLat)<sup>64, 65</sup> and assessed following harmonized procedures<sup>64, 65</sup> as in previous works.<sup>32, 40, 66-70</sup> Clinical diagnoses were established by neurodegenerative disease experts through an extensive neurological, neuropsychiatric, and neuropsychological examination comprising semi-structured interviews and standardized cognitive and functional assessments (**Table 2, Supplementary Material 1.2**). All participants with neurodegenerative conditions were in early/mild stages of the disease and did not fulfill criteria for other neurological disorders or specific psychiatric conditions. Neither did they present primary language deficits or a history of substance abuse. Participants with bvFTD were functionally impaired and exhibited prominent changes in personality and social behavior, as verified by caregivers. Participants with PD were medicated with antiparkinsonian therapy and evaluated during “on” phase. Participants with AD were also functionally impaired as verified by caregivers. Each neurodegenerative sample was comparable in sex, age, and years of formal education with HCs. The only significant difference in sex between bvFTD and HCs (**Table 2**) was controlled in all subsequent analyses. Finally, whole-brain GM was compared between each neurodegenerative group and HCs, showing a predominantly orbitofronto-cingulate-temporal atrophy in bvFTD<sup>18, 71, 72</sup>, no atrophy in PD,<sup>73-75</sup> and extended bilateral temporal with less extended fronto-parietal atrophy in AD<sup>76-78</sup> (**Supplementary Material 1.3; Supplementary Fig. 1**). The institutional ethics committee of each recruitment center approved the study protocol. All participants provided signed informed consent in accordance with the Declaration of Helsinki.

## Experimental protocol

All participants completed a multimodal assessment protocol including a behavioral SRL assessment, ongoing high-density EEG recordings, and an MRI session.

## Behavioral data: Socially reinforced learning task

We adapted an SRL task validated in a behavioral study with healthy persons.<sup>10</sup> By pressing predefined keys, participants were asked to judge the category membership “A” or “B” of three-digit numbers presented repeatedly across six cycles on a computer screen. Visual feedback immediately followed each number-category judgement (**Fig. 1A**). Participants were informed that there was no underlying rule defining the category membership of each number. Knowledge of the correct or incorrect outcome of previous category judgments for a particular number served to enhance performance over subsequent cycles. The task comprised two feedback conditions. In the SRL condition, socioemotional feedback was given a single face with one smiling and one angry expression for correct and incorrect responses, respectively.<sup>10</sup> The faces’ gender matched the participant’s gender. In the NSRL condition, feedback was given via green and red circles displayed for correct and incorrect responses, respectively. At the end of the experiment, participants were explicitly asked about the valence of each feedback type (**Table 3**). All groups presented adequate comprehension of these two factors (with no significant differences; for details see **Supplementary Material 2.1**). Each trial consisted of an initial stimulus (a three-digit number) presented in white color over a black background for 1500 ms, followed by a black screen (1000 ms) and then by categories’ options (“A” and “B”) positioned to the left and right of the screen over left/right arrows respectively. Participants had to respond by choosing a letter through the corresponding computer keyboard arrows with their dominant hand. Afterwards, another black screen was shown for a random period (between 2000 and 2500 ms). Finally, social or non-social feedback was provided for 1000 ms. Instructions and a set of two practice trials were presented before each block. The order of SRL/NSRL blocks alternated, with the first being social for half of the participants. Categories A or B were counterbalanced in a pseudorandom design across blocks. In total, participants completed six blocks (three SRL, three NSRL). Four different three-digit numbers (four trials) were repeated across six cycles per block. In total, 24 different numerical stimuli and 144 trials were run per subject. The number of trials did not change according to performance. For further details on the task design see **Supplementary Material 2.2**. Accuracy and response time data were collected for each trial. During the whole task, high-density EEG recordings were obtained to assess potential electrophysiological differences between SRL and NSRL modulations across groups (see below).



## EEG: Acquisition and signal preprocessing

Signals were acquired, for all participants, with a Biosemi Active-two 128 channel system at 1024 Hz. Data was re-referenced offline separately to linked mastoid electrodes, resampled at 512 Hz and filtered at 0.5-50  $\mu$ V. Eye movements or blink artifacts were corrected with independent component analysis<sup>79</sup> and with a visual inspection protocol.<sup>30, 32, 80-87</sup> Noisy epochs were rejected using an automatic EEGLAB procedure. Criteria for exclusion included elimination of trials which exceeded a threshold of 2.5 *SDs* from the mean probability distribution calculated from all trials and by measuring the kurtosis of probability distribution.<sup>88</sup> The percentage of rejected trials was similar across groups and conditions (**Supplementary Table 5.1** and **Supplementary Table 5.2**). EEG data was segmented into one-second epochs and baseline-corrected (-200 to 0 ms) for the feedback stimuli.

## Neuroimaging: Acquisition and preprocessing

MRI acquisition and pre-processing steps are reported as recommended by the Organization for Human Brain Mapping<sup>89, 90</sup> Acquisition parameters in each center followed standard protocols<sup>30, 32, 91</sup> (**Supplementary Material 6.1**). For neuroanatomical analysis, whole-brain T1-rapid anatomical three-dimensional gradient echo volumes were acquired. Sixteen three-dimensional volumetric images (from six HCs, three bvFTD, five PD and two AD participants) were excluded due to missing or artifactual data. The resulting subsamples were demographically matched in age and years of formal education. However, as regards sex, a significant difference was observed between bvFTD and HCs (**Supplementary Table 6.2**). These differences were controlled in the statistical analyses (see 'Statistical analysis' section).

For voxel-based morphometry (VBM) analysis, data were processed on the DARTEL Toolbox following validated procedures<sup>30, 66, 92</sup> via Statistical Parametric Mapping software (SPM12, <https://www.fil.ion.ucl.ac.uk/spm/software/spm12/>). T1-weighted images in native space were first segmented using the default parameters of the SPM12 (bias regularization was set to 0.001 and bias FWHM was set to 60-mm cut-off) into GM, white matter, and cerebrospinal fluid (these three tissues were used to estimate the total intracranial volume; TIV). DARTEL (create template) module was run later using the GM and white matter segmented images –following

SPM12 default parameters– to create a template that is generated from the complete data set (increasing the accuracy of inter-subject alignment).<sup>93</sup> Next, we used the “Normalize to MNI Space” module from DARTEL Tools to affine register the last template from the previous step into the MNI Space. This transformation was applied to all the individual GM segmented scans to also be brought into standard space. Subsequently, all images were modulated to correct volume changes by Jacobian determinants, and to avoid bias in the intensity of an area due to its expansion during warping. Finally, data were smoothed using a 10-mm full-width-at-half-maximum isotropic Gaussian kernel to accommodate for inter-subject differences in anatomy. The size of the kernel was selected based on previous recommendations.<sup>92, 94</sup>

To analyze the images of each center together and avoid a scanner effect in our results, the normalized and smoothed DARTEL outputs were transformed to  $w$ -score images.<sup>95-99</sup>  $W$ -scores, similar to  $z$ -scores (mean = 0,  $SD = 1$ ), represent the degree to which the observed GM volume in each voxel is higher or lower (positive or negative  $w$ -score) than expected, based on an individual's global composite score adjusted for specific covariates (age, disease, TIV and scanner type).  $W$ -scores were calculated dividing each participant's observed and predicted GM volume (residuals) by their  $SD$ . The resulting  $w$ -score maps of each subject were used for further statistical analyses.

## Statistical analysis

### Behavioral analysis: Socially reinforced learning task

First, we discarded trials with response latencies above 10 s (for details see **Supplementary Material 3.1**). Second, we excluded trials whose response time fell more than 3  $SD$ s away from each subject's mean.<sup>100</sup> The percentage of rejected trials was similar across groups and conditions (**Supplementary Table 3.2**). To validate the results in HCs, accuracy scores (the number of correct responses per cycle and per feedback condition) were calculated for each subject. To confirm the expected effect of learning (higher accuracy over successive cycles) and feedback type (higher accuracy in SRL than in NSRL condition) in HCs, we analyzed their performance through repeated measures ANOVA of accuracy scores across cycles and feedback condition. A Shapiro-Wilk test for normality on HCs accuracy evidenced normal distribution (**Supplementary Material 3.3**).

For each subject, we computed a learning index calculated as the Rho value of the Spearman correlation between accuracy and cycle number.<sup>101-103</sup> We obtained one learning index for each SRL and NSRL condition. This measure integrates the accuracy-by-cycle interaction in a slope index, allowing us to compare the learning process between conditions.<sup>101</sup> Performance was compared between feedback conditions via a one-way ANOVA for the learning index in HCs.

Next, the following procedure was designed to compare HCs and patients. To compare behavioral performance between groups, as normality and homoscedasticity assumptions were not fully met (**Supplementary Material 3.3** and **Supplementary Material 3.4**), nonparametric Kruskal-Wallis tests were conducted for the learning index (with two-tail Mann-Whitney-U tests for post hoc comparisons). As in previous reports with neurodegenerative diseases,<sup>30, 32, 104-106</sup> since our hypotheses hinged on differences between each neurodegenerative group and HCs, and given that demographic and behavioral features were not matched across neurodegenerative samples (bvFTD vs PD vs AD), we focused on pairwise comparisons between demographically matched tandems: HCs vs bvFTD, HCs vs PD, HCs vs AD (**Table 2**). In addition, given that a significant difference was found in sex between bvFTD and HCs, we conducted additional group comparison analyses of covariance using permutation testing controlling for sex<sup>107</sup> (**Supplementary Material 3.5**). Moreover, to rule out potential confounds of facial emotion recognition disturbances in bvFTD (particularly, for negative emotions),<sup>108, 109</sup> we also conducted additional group comparison analyses of covariance using permutation testing and controlling for feedback valence recognition (**Supplementary Material 3.6**). Finally, we carried out modified *t* tests<sup>110</sup> to estimate the percentage of impaired learning indexes in participants with neurodegenerative disease in contrast to HCs. This analysis allows to assess the percentage of cases that met criteria for dissociation between SRL and NSRL conditions (see **Supplementary Material 3.7** for details).

### **EEG: Spatiotemporal clustering associated to feedback**

To track ongoing markers of learning by feedback we targeted the MFN, characterized by a negative deflection over the midline frontal region of the scalp.<sup>53-55</sup> Here, we aimed to analyze the potential differences in MFN modulations of SRL vs. NSRL by comparing the spatiotemporal cluster for both feedback conditions for each group. Also, in order to assess early

vs. late learning modulation effects of ongoing MFN markers, we included an additional measure (initial vs. final set of trials), as previously done.<sup>111</sup> We compared the initial (first half) versus final (second half) set of trials per cycle of the social condition within each group. We used a split analysis applying the same MFN approach as it represents a direct measure of learning by feedback. The learning index is a dimensional measure of the slope of the behavioral correlation, and it does not directly represent an association with the MFN modulation by feedback. This way, we avoided problems related to (a) the Rho not being univariate, (b) inflating the number of comparisons between time points and electrodes due to single-trial analysis in a regression, and (c) controversial single-trial association between performance and ERP given the high level of noise,<sup>112</sup> as signal averaging approaches are less affected by artifacts and noise-related variability.<sup>113</sup> Given these considerations, and following similar approaches performed with the MFN<sup>111, 114</sup> and other ERPs,<sup>115, 116</sup> we evaluated the learning effects using a MFN split analysis.

To avoid *a priori* spatiotemporal bias, nonparametric data-driven spatiotemporal clustering<sup>117</sup> was implemented on Matlab software with the Fieldtrip Toolbox (version 20180313), with one-tailed paired *t*-tests as univariate tests. This nonparametric clustering method was introduced to address the resulting multiple comparisons problem.<sup>118</sup> The *t*-values of adjacent spatiotemporal points with  $P < 0.05$  were clustered together by summing their *t*-values, and the largest cluster was retained. A minimum of 10 neighboring electrodes were required to pass this threshold and form a robust cluster.<sup>119</sup> The cluster-level *t*-value was calculated as the sum of the individual *t*-values at the points within the cluster. To assess the significance of a spatiotemporal cluster identified above, this procedure was repeated 5000 times, with recombination and randomized resampling of the subject-wise averages before each repetition using a Monte Carlo method.<sup>120</sup> After each repetition, the *t*-value of the largest cluster identified was retained. The proportion of these 5000 randomized *t*-values greater than the originally identified cluster-level *t*-value was used to calculate a nonparametric *P* value for the originally identified cluster. This approach avoids the problem of multiple comparisons across the dimensions of electrode, time, and space.<sup>117, 119</sup>

## Neuroimaging: VBM analysis

Regression analyses were performed to assess the association between GM volume and behavioral performance (SRL and NSRL learning indexes) via non-parametric permutation tests on Statistical non-parametric Mapping (SnPM13, <http://www.nisox.org/Software/SnPM13/>, 5000 random permutations, cluster-forming threshold set at 0.001) toolbox for SPM12. Permutation tests outperform parametric tests in correction for multiple comparisons.<sup>121</sup> Sex was included as a covariate of no interest. In order to increase behavioral variance and statistical power by increasing sample size,<sup>39, 122-124</sup> we used two approaches collapsing different groups. First, we performed analyses including all four groups (HCs, bvFTD, PD and AD), to assess a general association between brain correlates of performance. Second, each pathological group was analyzed in tandem with healthy controls (bvFTD-HCs, PD-HCs, and AD-HCs) to evaluate specific performance-related neuroanatomical correlates, following recent neurodegenerative studies.<sup>30, 32, 125-128</sup> To adjust for multiple comparisons, we used cluster-wise inference with family-wise error (FWE) rate correction of  $P\text{-FWE} < 0.05$ .<sup>129, 130</sup> Finally, a conjunction analysis was performed in order to assess the extent of shared/distinct neural correlates of SRL and NSRL conditions. We used Imcalc in SPM12, to assess the conjoint analysis of grey matter volume and the two learning indexes in all groups together with corrected thresholded maps ( $P\text{-FWE} < 0.05$ ). The binarized images were used to obtain a conjunction map using the equation:  $i1 + (2*i2)$ .<sup>131, 132</sup>

## Data availability

Anonymized data that support the study findings are available in open-source software<sup>133</sup> or from the corresponding author upon reasonable request.

## Results

### Behavioral results

In HCs, accuracy improved across cycles, even when assessing SRL and NSRL conditions separately. Moreover, accuracy was higher in the SRL than in the NSRL condition (**Fig. 1B** and **Supplementary Material 4**). In this line, performance was also compared between feedback conditions for the learning index, revealing a significant difference between SRL

(mean = 0.47,  $SD = 0.36$ ) and NSRL (mean = 0.21,  $SD = 0.46$ ) feedback conditions ( $F_{(1,39)} = 8.49$ ,  $P = 0.005$ ,  $\eta^2 = 0.17$ ) (**Fig. 1B**) in HCs.

Moreover, the learning index was used to assess between-group comparisons. A significant main effect of group was observed for the learning index in SRL and in NSRL conditions (**Table 4**).

When comparing the learning index between each neurodegenerative sample and HCs separately, we found that participants with bvFTD performed significantly worse in the SRL condition, but not in NSRL condition. The same pattern was observed in participants with PD. Finally, AD showed impaired learning in both conditions relative to HCs (**Table 4** and **Fig. 1C**). Behavioral results were replicated when controlling for sex (see **Supplementary Material 3.5** for details) and valence recognition (see **Supplementary Material 3.6** for details).

## EEG results: Spatiotemporal clusters of MFN

Significant spatiotemporal clusters were observed for the SRL vs NSRL comparison in all groups. As expected, HCs showed MFN modulation in a significant frontal cluster ( $t\text{-sum} = -37180.09$ ,  $P = 0.001$ ), with more negative modulation during the SRL than the NSRL condition. Participants with bvFTD presented no frontal modulation by condition, but they exhibited a small significant posterior (occipital) cluster ( $t\text{-sum} = -4700.34$ ,  $P = 0.003$ ) with more negative voltage during social condition and maximum  $t$ -value soon after stimulus onset (170 ms). Conversely, the PD group exhibited a significant frontal cluster ( $t\text{-sum} = -87355.85$ ,  $P = 0.001$ ) in the same direction as HCs, with maximum  $t$ -value at 334 ms. The AD group also showed a significant frontal cluster ( $t\text{-sum} = -30859.08$ ,  $P = 0.004$ ), with more negative voltage for the SRL condition and its maximum  $t$ -value at 412 ms (**Fig. 2A**).

Concerning the effect of learning at neural levels across task cycles, the comparison between initial and final set during the SRL condition was significant for HCs ( $t\text{-sum} = -6990.78$ ,  $P = 0.036$ ), with its maximum  $t$ -value at 246 ms, and with an expected more negative voltage (associated with enhanced learning) for the final trials in frontal regions. This effect was not observed in any neurodegenerative group (**Fig. 2B**).

## Neuroimaging results: Brain-behavior associations

When considering all groups, higher performance in SRL was associated with greater volume of temporo-parietal cortices (right superior temporal, supramarginal and postcentral), fronto-limbic regions (right inferior frontal operculum, fusiform, and parahippocampal areas; left insula and precentral; bilateral thalamus, and middle cingulate areas), and bilateral middle occipital areas (**Fig. 3, first row left, Supplementary Table 6.3**). Contrarily, higher NSRL performance was associated with greater GM volume of the bilateral hippocampus (**Fig. 3, first row right, Supplementary Table 6.4**).

In the bvFTD group, significant associations emerged between higher performance in SRL and greater volume of predominantly temporo-parietal regions were found (including left superior and middle temporal, bilateral precuneus, fusiform and inferior posterior areas) (**Fig. 3, second row left, Supplementary Table 6.3**). NSRL was associated with greater volume of the right hippocampus and the middle temporal pole (**Fig. 3 second row right, Supplementary Table 6.4**).

In the PD group, no significant associations between GM volume and performance were found. In the AD group showed associations between higher SRL performance and greater GM volume of predominantly limbic regions (right inferior and superior orbitofrontal, anterior cingulate and hippocampus; left precentral, inferior frontal operculum, insula, middle temporal; and bilateral fusiform - **Fig. 3, third row left, Supplementary Table 6.3**). NSRL was associated with greater right hippocampus and middle temporal pole GM volume (**Fig. 3, third row right, Supplementary Table 6.4**).

Finally, conjunction analysis of SRL and NSRL conditions (**Fig. 4**) in all groups revealed small overlapping clusters in the right parahippocampus (peak MNI coordinate:  $x = 22.5$ ;  $y = -22.5$ ;  $z = -15$ ;  $k = 292$ ) and right hypothalamus (peak MNI coordinate:  $x = 15$ ;  $y = -4.5$ ;  $z = -10.5$ ;  $k = 224$ ).

## Discussion

We investigated multimodal markers of SRL and NSRL across healthy participants and neurodegenerative diseases. As expected, social feedback enhanced learning in HCs. This effect was specifically impaired in bvFTD and PD, while AD presented generalized learning

disruptions. HCs showed the expected pattern of increased MFN modulation during SRL compared to NSRL. This effect was not observed in bvFTD. For SRL learning effects (comparing initial and final cycles of the task), HCs exhibited greater MFN modulation for final trials. This MFN differentiation was not seen in any neurodegenerative group. Neuroanatomical correlates of SRL showed extended temporo-parietal and fronto-limbic hubs in all groups, as well as associations with specific temporo-parietal regions in bvFTD, and predominantly fronto-limbic regions in AD. In contrast, NSRL was consistently linked to medial temporal regions and in particular with hippocampus. No association between task performance and brain atrophy was observed in PD. Together, these multimodal findings reveal mechanisms of learning and social feedback in SRL across different pathophysiological lesion models sensitive to SRL (bvFTD and PD) and generalized learning deficits (AD).

## **Behavioral social-feedback facilitation and neurodegenerative profiles**

The learning gains of HCs following social feedback<sup>10, 13</sup> were disrupted in bvFTD and PD (in their corresponding comparison with controls). While learning from non-social feedback appeared generally unimpaired in these groups in comparison with controls, the addition of social feedback did not enhance learning. This suggests social cognition deficits impair learning in both diseases,<sup>40, 44</sup> but based on the existing literature, coupled with our novel multimodal imaging findings, there is reason to suspect these deficits may arise from different cognitive processes. In bvFTD, primary social cognitive deficits<sup>18, 36-38, 40</sup> may prevent the integration of social information during decision-making processes, disrupting associative learning.<sup>33, 36</sup> This might mirror the way that memory impairments in bvFTD<sup>47, 51, 124, 134, 135</sup> are thought to be explained (in this task) by social cognition deficits. Interestingly, in PD, the interaction of feedback-based learning<sup>41</sup> and socioemotional deficits<sup>44</sup> (particularly facial processing)<sup>46</sup> may explain this group's selective SRL disruptions. These potential explanations of behavioral deficits pointing to different physiopathological processes seems to be supported by their brain temporal and spatial signatures (see below). In contrast to these diseases, the generalized impairments across both feedback conditions observed in AD are likely explained by domain-general associative learning decline<sup>136</sup> and object memory alterations.<sup>137, 138</sup> Both processes may prevent the integration and maintenance of relevant feedback information.



Altogether, behavioral findings parallel clinical patterns of social (bvFTD and PD) and associative learning (AD) disruptions.

## **Ongoing cortical correlates of SRL as bvFTD specific markers**

Online MFN modulations evidenced both correlates of learning<sup>53, 56, 57</sup> and social-feedback facilitation in HCs<sup>58, 139, 140</sup> (but see).<sup>35</sup> The selective abolishment on social MFN modulations in bvFTD in comparison with controls, beyond preserved low-level distinction of facial stimulus processing (posterior cluster resembling learning-unrelated N170),<sup>141</sup> may be indicative of specific alterations in social prediction-error signal coding. Abnormal social processing may impact action-reward and contextual updating.<sup>142</sup> Indeed, social predictive-error coding is partially indexed by fronto-cingulate mechanisms,<sup>142</sup> compromised in people with bvFTD. In contrast, altered learning MFN modulations in PD, compatible with fronto-striatal disruptions<sup>143</sup> may evidence subtle pathophysiological mechanisms of feedback-related learning deficits. In AD, disrupted learning MFN modulations<sup>144</sup> may resemble generalized associative learning alterations<sup>136, 137</sup> in accordance to our hypothesis. Thus, the MFN may be considered a novel ongoing marker of SRL in neurodegeneration, selectively compromised in bvFTD.

## **Neuroanatomical markers of SRL and atrophy mechanisms**

Neuroanatomical correlates of SRL suggest that the integration of social and learning processes critically relies on temporo-parietal hubs (i.e., temporo-parietal junction)<sup>24</sup> and secondarily on fronto-insular-limbic regions, consistent with predictions from the social-context network model.<sup>17-22</sup> These hubs index critical processes for socio-contextual learning,<sup>145</sup> including perspective taking, facial emotional recognition, contextual integration, reward processing, and object memory. In bvFTD, neuroanatomical signatures of SRL support the role of the temporo-parietal junction in processing behaviorally relevant social information.<sup>146</sup> Perspective taking in socially-motivated contexts may also contribute to associative learning and object memory processes.<sup>36</sup> Conversely, in AD, specific limbic involvement in SRL suggests its role in the use of social cues during associative learning. In particular, associations with hippocampal regions may reflect the involvement of general associative learning and object memory processes.<sup>147</sup> Moreover, additional associations with orbitofrontal, insular, and anterior cingulate regions

may indicate socio-emotional and reward-related processing.<sup>22, 145, 148-150</sup> Lack of neuroanatomical associations in PD suggests specific SRL deficits may be explained by pathophysiological mechanisms unrelated with brain atrophy.<sup>143</sup>

Compared with SRL, NSRL was consistently associated with medial temporal (hippocampal) regions<sup>6, 59</sup> in HCs, bvFTD and AD. In this sense, conjunction analysis suggests large differential anatomical correlates for social and non-social conditions, with minimum overlap. Expected regions involved in general associative and implicit learning such as hippocampus<sup>151, 152</sup> and hypothalamus<sup>153</sup> evidenced common neural correlates for both social and non-social learning. In sum, cortical temporo-parietal hubs (and, to a lesser extent, fronto-limbic regions) may play a key role in SRL and in selective bvFTD deficits.

## **Multimodal evidence of distinct mechanisms across neurodegenerative disorders**

Our study provides novel multimodal evidence of distinct social and learning processes in neurodegenerative diseases. Ongoing frontal EEG markers and brain structural correlates, captured by the social context network model, shed light on how similar SRL deficits in different diseases may be rooted in distinct anatomo-functional disruptions. Neurophysiological evidence of broad temporo-parietal and frontal involvement in the SRL condition compared to NSRL points to the complexity of social sources of feedback. Results from bvFTD patients, in comparison with controls, reveal selective social deficits consistent across dimensions. Their failure to use socially relevant information as a prior to correct inferential prediction errors and improve learning<sup>18, 39, 40</sup> might be related to both neurodegeneration and a lack of appropriate MFN modulations. This lack of social reward mediation in updating expectations and actions could hardly be explained by a perceptual impairment, since visuoperceptual integration of stimuli seems to be preserved (supported by N170 component modulation<sup>154</sup> and SRL deficits when covarying by valence recognition). Consistent with our findings, prior research has shown that social signals are encoded by the temporo-parietal junction, anterior cingulate, and dorsomedial prefrontal cortices.<sup>24, 142</sup> Although future research is needed to test this conjecture, our findings in bvFTD could be explained by alterations in social prediction-error coding. Moreover, these deficits likely exacerbate memory impairments also present in this condition.<sup>47, 51, 134, 135</sup> Deficits in PD were

accompanied by preserved social MFN and impaired learning MFN modulations, as well as a lack of neuroanatomical specificity, suggesting a different pathophysiological mechanism. Specifically, possible MFN-related fronto-striatal dysregulations<sup>143</sup> may impact social reward prediction-error signals during feedback-related learning.<sup>3, 26, 155</sup> Finally, social MFN modulations and fronto-limbic associations in AD could be impacted by disrupted associative learning and object memory processes in SRL. These mechanisms are strongly affected by medial temporal and temporo-parietal degeneration.<sup>156</sup> Consequently, social-feedback learning facilitation may be vulnerable to decay with increasing disease severity.<sup>36</sup> Between-condition comparisons in each neurodegenerative group fall outside the scope of our study. However, multidimensional results coupled with supplementary dissociation analysis between conditions among neurodegenerative cases (see **Supplementary Material 3.7** for details), partially support the interpretation of different social and learning mechanisms, pointing to more specific SRL disruptions in bvFTD.

This convergent evidence of SRL patterns across neurodegenerative diseases carries clinical implications. Social cognitive disruptions and memory alterations have been largely described as canonical deficits in bvFTD and AD, respectively. However, evidence of memory impairments in bvFTD<sup>49</sup> and social cognitive deficits in AD<sup>50</sup> has hindered differential diagnosis between both conditions.<sup>47, 51</sup> Here we shed light on this issue by combining social cognition and learning processes in a single task, and using multiple levels of analysis including EEG and MRI. Our multimodal findings present two disrupted SRL patterns in bvFTD and AD. Moreover, they revealed how similar behavioral SRL outcomes (i.e., in bvFTD and PD) may be explained by different neurophysiological pathways. Our study acknowledges the synergic assessment of these cognitive processes<sup>19-22, 157</sup> as well as the specificities of each model in their comparison to HCs, offering new transnosological insights across neurodegenerative conditions.

## Limitations and further research

We acknowledge certain limitations to our study. First, our design is based on a modest sample size. Nevertheless, it is similar to or larger than those of other multimodal reports assessing neurodegenerative subtypes.<sup>30, 32, 36, 40, 158, 159</sup> Also, this caveat was counteracted by the strict control of demographic and clinical variables, as well as detailed diagnostic procedures and

systematic assessments. Moreover, our multimodal results across behavioral, electrophysiological, and neuroanatomical dimensions, with moderate to large effect sizes, further attests to their robustness. In any case, future studies should replicate and extend these results with larger and adequately matched patient groups and alternative designs allowing for exploration of systematic effects across different neurodegenerative groups. Such an approach may allow for direct patients group comparisons which are beyond the scope of our study. Second, our findings rely on social-feedback facilitation processes triggered by static emotional faces. Performance was assessed through implicit associations including simple stimuli (three-digit numbers) to prevent semantic confounds and task-load effects on learning outcomes.<sup>160, 161</sup> The use of simple stimuli allows assessing cognitively impaired populations. Notwithstanding, future tasks should strive for greater ecological validity by addressing SRL using more naturalistic settings<sup>33, 34</sup> and stimuli (such as sentences or object localization associations). Third, the processing of socioemotional stimuli in the SRL may be affected by facial emotion recognition disturbances that are characteristic of bvFTD.<sup>108, 109</sup> However, we used a single face displaying only two emotions and our results persisted when controlling for valence recognition (**Supplementary Material 2.1** and **Supplementary Material 3.6**). These results suggest that feedback processing is influenced by social content (rather than emotional detection impairments). Future studies should compare how learning is affected by different social stimuli (facial vs. non-facial, and emotional vs. non-emotional). In this sense, learning effects between conditions may be influenced by visuo-perceptual complexity of feedback cues. However, several reasons suggest that the observed effects are better explained by the social nature of the SRL stimulus including the robustness of an already validated task<sup>10</sup> similar to previous experimental designs,<sup>6, 33, 38</sup> cognitive load control with the use of one face per valence,<sup>35</sup> MFN modulations suggesting processing of learning effects instead to stimulus complexity (except for bvFTD), and replication of results after controlling for valence recognition (**Supplementary Material 3.6**; see also **Supplementary Discussion 7**). Nonetheless, visuo-perceptual complexity among stimuli should be better controlled in future works, with a 2x2 (social/non-social, complex/simple) stimuli design. Finally, although our multimodal assessment approach includes task-related EEG measures, future studies should also include active functional neuroimaging paradigms to better elucidate the regions and networks mediating SRL.

## Conclusions

Our multimodal lesion model approach reveals convergent evidence of dissociable effects of learning and social feedback across neurodegenerative diseases. These novel results may support theoretical accounts of multimodal SRL mechanisms involving ongoing MFN activity and anatomical deficits underpinned by the social-context network model. A novel clinical agenda is thus opened, related to the characterization and treatment of these social cognition and learning processes in neurodegeneration.

## Acknowledgments

We thankfully acknowledge the collaboration of Instituto Conci Carpinella (Córdoba, Argentina) and Hospital Nacional de Clínicas (Facultad de Ciencias Médicas, Universidad Nacional de Córdoba, Córdoba, Argentina). Finally, we thank the participants and their families for their invaluable time and commitment to our study.

## Funding

This work is partially supported by grants from Takeda CW2680521; CONICET; ANID/FONDECYT Regular (1210195 and 1210176); FONCYT-PICT 2017-1820; ANID/FONDAP/15150012; Sistema General de Regalías (BPIN2018000100059), Universidad del Valle (CI 5316); Programa Interdisciplinario de Investigación Experimental en Comunicación y Cognición (PIIECC), Facultad de Humanidades, USACH; Alzheimer's Association GBHI ALZ UK-20-639295; and the MULTI-PARTNER CONSORTIUM TO EXPAND DEMENTIA RESEARCH IN LATIN AMERICA [ReDLat, supported by National Institutes of Health, National Institutes of Aging (R01 AG057234), Alzheimer's Association (SG-20-725707), Rainwater Charitable foundation - Tau Consortium, and Global Brain Health Institute)]. The contents of this publication are solely the responsibility of the authors and do not represent the official views of these Institutions.

## Competing interests

The authors report no competing interests.

## Supplementary material

Supplementary material is available at *Brain* online.

## References

1. Martin J, Rychlowska M, Wood A, Niedenthal P. Smiles as multipurpose social signals. *Trends in cognitive sciences*. 2017;21(11):864-877.
2. Verneti A, Smith TJ, Senju A. Gaze-contingent reinforcement learning reveals incentive value of social signals in young children and adults. *Proceedings of the Royal Society B: Biological Sciences*. 2017;284(1850):20162747.
3. Kruppa JA, Gossen A, Weiß EO, et al. Neural modulation of social reinforcement learning by intranasal oxytocin in male adults with high-functioning autism spectrum disorder: a randomized trial. *Neuropsychopharmacology*. 2019;44(4):749-756.
4. Zaki J, Kallman S, Wimmer GE, Ochsner K, Shohamy D. Social cognition as reinforcement learning: feedback modulates emotion inference. *J Cogn Neurosci*. 2016;28(9):1270-1282.
5. Lin A, Adolphs R, Rangel A. Impaired learning of social compared to monetary rewards in autism. *Frontiers in neuroscience*. 2012;6:143.
6. Mihov Y, Mayer S, Musshoff F, Maier W, Kendrick KM, Hurlmann R. Facilitation of learning by social-emotional feedback in humans is beta-noradrenergic-dependent. *Neuropsychologia*. 2010;48(10):3168-3172.
7. Colombo M, Stankevicius A, Seriès P. Benefits of social vs. non-social feedback on learning and generosity. Results from the Tipping Game. *Frontiers in Psychology*. 2014;5:1154.
8. Lee J, Green MF. Social preference and glutamatergic dysfunction: underappreciated prerequisites for social dysfunction in schizophrenia. *Trends Neurosci*. 2016;39(9):587-596.
9. Heerey EA. Learning from social rewards predicts individual differences in self-reported social ability. *J Exp Psychol Gen*. 2014;143(1):332.

10. Hurlemann R, Patin A, Onur OA, et al. Oxytocin enhances amygdala-dependent, socially reinforced learning and emotional empathy in humans. *J Neurosci*. 2010;30(14):4999-5007. doi:10.1523/JNEUROSCI.5538-09.2010
11. Olsson A, Phelps EA. Social learning of fear. *Nat Neurosci*. 2007;10(9):1095-1102.
12. Gariépy J-F, Watson KK, Du E, et al. Social learning in humans and other animals. *Frontiers in neuroscience*. 2014;8:58.
13. Ferdinand NK, Hilz M. Emotional feedback ameliorates older adults' feedback-induced learning. *PloS one*. 2020;15(4):e0231964.
14. Fareri DS, Delgado MR. Social rewards and social networks in the human brain. *The neuroscientist*. 2014;20(4):387-402.
15. LaBar KS, Cabeza R. Cognitive neuroscience of emotional memory. *Nature Reviews Neuroscience*. 2006;7(1):54-64.
16. Tyng CM, Amin HU, Saad MN, Malik AS. The influences of emotion on learning and memory. *Frontiers in psychology*. 2017;8:1454.
17. Baez S, García AM, Ibanez A. The social context network model in psychiatric and neurological diseases. *Social Behavior from Rodents to Humans*. Springer; 2016:379-396.
18. Ibanez A, Manes F. Contextual social cognition and the behavioral variant of frontotemporal dementia. *Neurology*. 2012;78(17):1354-62. doi:10.1212/WNL.0b013e3182518375
19. Ibáñez A, García AM. *Contextual cognition: the sensus communis of a situated mind*. Springer; 2018.
20. Ibáñez A. Brain oscillations, inhibition and social inappropriateness in frontotemporal degeneration. *Brain*. 2018;141(10):e73-e73.
21. Ibáñez A, Billeke P, de la Fuente L, Salamone P, García AM, Melloni M. Reply: towards a neurocomputational account of social dysfunction in neurodegenerative disease. *Brain*. 2017;140(3):e15-e15.
22. Ibanez A, Schulte M. Situated minds: conceptual and emotional blending in neurodegeneration and beyond. *Brain*. 2021;143(12):3523-3525. doi:10.1093/brain/awaa392
23. Decety J, Lamm C. The role of the right temporoparietal junction in social interaction: how low-level computational processes contribute to meta-cognition. *The neuroscientist*. 2007;13(6):580-593.
24. Joiner J, Piva M, Turrin C, Chang SW. Social learning through prediction error in the brain. *NPJ science of learning*. 2017;2(1):1-9.

25. Hu J, Qi S, Becker B, et al. Oxytocin selectively facilitates learning with social feedback and increases activity and functional connectivity in emotional memory and reward processing regions. *Hum Brain Mapp.* 2015;36(6):2132-46. doi:10.1002/hbm.22760
26. Lin A, Adolphs R, Rangel A. Social and monetary reward learning engage overlapping neural substrates. *Soc Cogn Affect Neurosci.* 2012;7(3):274-81. doi:10.1093/scan/nsr006
27. Evans S, Fleming SM, Dolan RJ, Averbeck BB. Effects of emotional preferences on value-based decision-making are mediated by mentalizing and not reward networks. *J Cogn Neurosci.* 2011;23(9):2197-2210.
28. Rorden C, Karnath HO. Using human brain lesions to infer function: a relic from a past era in the fMRI age? *Nature reviews Neuroscience.* 2004;5(10):813-9. doi:10.1038/nrn1521
29. Baez S, Couto B, Torralva T, et al. Comparing moral judgments of patients with frontotemporal dementia and frontal stroke. *JAMA neurology.* 2014;71(9):1172-6. doi:10.1001/jamaneurol.2014.347
30. Garcia-Cordero I, Sedeno L, de la Fuente L, et al. Feeling, learning from and being aware of inner states: interoceptive dimensions in neurodegeneration and stroke. *Philos Trans R Soc Lond B Biol Sci.* 2016;371(1708)doi:10.1098/rstb.2016.0006
31. Garcia-Cordero I, Sedeno L, Fraiman D, et al. Stroke and Neurodegeneration Induce Different Connectivity Aberrations in the Insula. *Stroke.* 2015;46(9):2673-7. doi:10.1161/STROKEAHA.115.009598
32. Salamone PC, Legaz A, Sedeño L, et al. Interoception primes emotional processing: Multimodal evidence from neurodegeneration. *J Neurosci.* 2021;41(19):4276-4292.
33. Keri S. Social influence on associative learning: double dissociation in high-functioning autism, early-stage behavioural variant frontotemporal dementia and Alzheimer's disease. *Cortex.* 2014;54:200-9. doi:10.1016/j.cortex.2014.02.018
34. Duff MC, Gallegos DR, Cohen NJ, Tranel D. Learning in Alzheimer's disease is facilitated by social interaction. *J Comp Neurol.* 2013;521(18):4356-69. doi:10.1002/cne.23433
35. Beston PJ, Barbet C, Heerey EA, Thierry G. Social feedback interferes with implicit rule learning: Evidence from event-related brain potentials. *Cognitive, Affective, & Behavioral Neuroscience.* 2018;18(6):1248-1258.
36. Wong S, Irish M, O'Callaghan C, et al. Should I trust you? Learning and memory of social interactions in dementia. *Neuropsychologia.* 2017;104:157-167.



37. Kumfor F, Irish M, Hodges JR, Piguet O. The orbitofrontal cortex is involved in emotional enhancement of memory: evidence from the dementias. *Brain*. 2013;136(10):2992-3003.
38. Perry DC, Sturm VE, Wood KA, Miller BL, Kramer JH. Divergent processing of monetary and social reward in behavioral variant frontotemporal dementia and Alzheimer's disease. *Alzheimer Dis Assoc Disord*. 2015;29(2):161.
39. O'Callaghan C, Bertoux M, Irish M, et al. Fair play: social norm compliance failures in behavioural variant frontotemporal dementia. *Brain*. 2016;139(1):204-216.
40. Melloni M, Billeke P, Baez S, et al. Your perspective and my benefit: multiple lesion models of self-other integration strategies during social bargaining. *Brain*. 2016;139(11):1-19.
41. Meissner SN, Südmeyer M, Keitel A, Pollok B, Bellebaum C. Facilitating effects of deep brain stimulation on feedback learning in Parkinson's disease. *Behav Brain Res*. 2016;313:88-96.
42. Schmitt-Eliassen J, Ferstl R, Wiesner C, Deuschl G, Witt K. Feedback-based versus observational classification learning in healthy aging and Parkinson's disease. *Brain Res*. 2007;1142:178-188.
43. Shohamy D, Myers C, Grossman S, Sage J, Gluck M, Poldrack R. Cortico-striatal contributions to feedback-based learning: Converging data from neuroimaging and neuropsychology. *Brain*. 2004;127(4):851-859.
44. Argaud S, Vérin M, Sauleau P, Grandjean D. Facial emotion recognition in Parkinson's disease: a review and new hypotheses. *Mov Disord*. 2018;33(4):554-567.
45. Baez S, Herrera E, Trujillo C, et al. Classifying Parkinson's disease patients with syntactic and socio-emotional verbal measures. *Frontiers in aging neuroscience*. 2020;12.
46. Ho MW-R, Chien SH-L, Lu M-K, et al. Impairments in face discrimination and emotion recognition are related to aging and cognitive dysfunctions in Parkinson's disease with dementia. *Scientific reports*. 2020;10(1):1-8.
47. Bertoux M, de Souza L, O'Callaghan C, et al. Social cognition deficits: the key to discriminate behavioral variant frontotemporal dementia from Alzheimer's disease regardless of amnesia? *Journal of Alzheimer's Disease*. 2016;49(4):1065-1074.
48. Shany-Ur T, Rankin KP. Personality and social cognition in neurodegenerative disease. *Curr Opin Neurol*. 2011;24(6)
49. Bertoux M, Flanagan EC, Hobbs M, et al. Structural Anatomical Investigation of Long-Term Memory Deficit in Behavioral Frontotemporal Dementia. *Journal of Alzheimer's Disease*. 2018;62(4):1887-1900. doi:10.3233/jad-170771

50. Strikwerda-Brown C, Ramanan S, Irish M. Neurocognitive mechanisms of theory of mind impairment in neurodegeneration: a transdiagnostic approach. *Neuropsychiatric disease and treatment*. 2019;15:557.
51. Hornberger M, Piguet O. Episodic memory in frontotemporal dementia: a critical review. *Brain*. 2012;135(3):678-692.
52. Seeley WW, Allman JM, Carlin DA, et al. Divergent social functioning in behavioral variant frontotemporal dementia and Alzheimer disease: reciprocal networks and neuronal evolution. *Alzheimer Dis Assoc Disord*. 2007;21(4):S50-S57.
53. Van Der Helden J, Boksem MA. Medial frontal negativity reflects learning from positive feedback. *Psychophysiology*. 2012;49(8):1109-1113.
54. Van Noordt SJ, Campopiano A, Segalowitz SJ. A functional classification of medial frontal negativity ERPs: Theta oscillations and single subject effects. *Psychophysiology*. 2016;53(9):1317-1334.
55. Yeung N, Sanfey AG. Independent coding of reward magnitude and valence in the human brain. *J Neurosci*. 2004;24(28):6258-6264.
56. Luft CDB. Learning from feedback: the neural mechanisms of feedback processing facilitating better performance. *Behav Brain Res*. 2014;261:356-368.
57. de Bruijn ER, Mars RB, Hester R. Processing of performance errors predicts memory formation: Enhanced feedback-related negativities for corrected versus repeated errors in an associative learning paradigm. *Eur J Neurosci*. 2020;51(3):881-890.
58. Pfabigan DM, Han S. Converging electrophysiological evidence for a processing advantage of social over nonsocial feedback. *Cognitive, Affective, & Behavioral Neuroscience*. 2019;19(5):1170-1183.
59. Onur OA, Schlaepfer TE, Kukulja J, et al. The N-methyl-D-aspartate receptor co-agonist D-cycloserine facilitates declarative learning and hippocampal activity in humans. *Biol Psychiatry*. 2010;67(12):1205-1211.
60. Rascovsky K, Hodges JR, Knopman D, et al. Sensitivity of revised diagnostic criteria for the behavioural variant of frontotemporal dementia. *Brain*. 2011;134(9):2456-77. doi:10.1093/brain/awr179
61. Hughes AJ, Daniel SE, Kilford L, Lees AJ. Accuracy of clinical diagnosis of idiopathic Parkinson's disease: a clinico-pathological study of 100 cases. *Journal of neurology, neurosurgery, and psychiatry*. Mar 1992;55(3):181-4.

62. Dubois B, Feldman HH, Jacova C, et al. Research criteria for the diagnosis of Alzheimer's disease: revising the NINCDS–ADRDA criteria. *The Lancet Neurology*. 2007;6(8):734-746.
63. McKhann GM, Knopman DS, Chertkow H, et al. The diagnosis of dementia due to Alzheimer's disease: Recommendations from the National Institute on Aging-Alzheimer's Association workgroups on diagnostic guidelines for Alzheimer's disease. *Alzheimer's & dementia*. 2011;7(3):263-269.
64. Ibáñez A, Pina-Escudero SD, Possin KL, et al. Dementia caregiving across Latin America and the Caribbean and brain health diplomacy. *The Lancet Healthy Longevity*. 2021;2(4):e222-e231.
65. Ibanez A, Yokoyama JS, Possin KL, et al. The Multi-Partner Consortium to Expand Dementia Research in Latin America (ReDLat): Driving Multicentric Research and Implementation Science. *Frontiers in neurology*. 2021;12:303.
66. Sedeno L, Piguet O, Abrevaya S, et al. Tackling variability: A multicenter study to provide a gold-standard network approach for frontotemporal dementia. *Hum Brain Mapp*. 2017;38(8):3804-3822. doi:10.1002/hbm.23627
67. Donnelly-Kehoe PA, Pascariello GO, García AM, et al. Robust automated computational approach for classifying frontotemporal neurodegeneration: Multimodal/multicenter neuroimaging. *Alzheimer's & Dementia: Diagnosis, Assessment & Disease Monitoring*. 2019;11(C):588-598.
68. Baez S, Manes F, Huepe D, et al. Primary empathy deficits in frontotemporal dementia. *Front Aging Neurosci*. 2014;6:262.
69. Moguilner S, García AM, Perl YS, et al. Dynamic brain fluctuations outperform connectivity measures and mirror pathophysiological profiles across dementia subtypes: a multicenter study. *Neuroimage*. 2020:117522.
70. Ibáñez A, Fittipaldi S, Trujillo C, et al. Predicting and Characterizing Neurodegenerative Subtypes with Multimodal Neurocognitive Signatures of Social and Cognitive Processes. *Journal of Alzheimer's disease : JAD*. Jul 15 2021;doi:10.3233/jad-210163
71. Piguet O, Hornberger M, Mioshi E, Hodges JR. Behavioural-variant frontotemporal dementia: diagnosis, clinical staging, and management. *The Lancet Neurology*. 2011;10(2):162-172.

72. Whitwell JL, Przybelski SA, Weigand SD, et al. Distinct anatomical subtypes of the behavioural variant of frontotemporal dementia: a cluster analysis study. *Brain*. 2009;132(11):2932-2946.
73. Huber SJ, Shuttleworth EC, Christy JA, Chakeres DW, Curtin A, Paulson GW. Magnetic resonance imaging in dementia of Parkinson's disease. *J Neurol Neurosurg Psychiatry*. 1989;52(11):1221-1227.
74. Schulz JB, Skalej M, Wedekind D, et al. Magnetic resonance imaging–based volumetry differentiates idiopathic Parkinson's syndrome from multiple system atrophy and progressive supranuclear palsy. *Annals of Neurology: Official Journal of the American Neurological Association and the Child Neurology Society*. 1999;45(1):65-74.
75. Price S, Paviour D, Scahill R, et al. Voxel-based morphometry detects patterns of atrophy that help differentiate progressive supranuclear palsy and Parkinson's disease. *Neuroimage*. 2004;23(2):663-669.
76. Du A-T, Schuff N, Kramer JH, et al. Different regional patterns of cortical thinning in Alzheimer's disease and frontotemporal dementia. *Brain*. 2007;130(4):1159-1166.
77. Pini L, Pievani M, Bocchetta M, et al. Brain atrophy in Alzheimer's Disease and aging. *Ageing research reviews*. 2016;30:25-48.
78. Landin-Romero R, Kumfor F, Leyton CE, Irish M, Hodges JR, Piguet O. Disease-specific patterns of cortical and subcortical degeneration in a longitudinal study of Alzheimer's disease and behavioural-variant frontotemporal dementia. *Neuroimage*. 2017;151:72-80.
79. Kim D, Kim S-K. Comparing patterns of component loadings: Principal Component Analysis (PCA) versus Independent Component Analysis (ICA) in analyzing multivariate non-normal data. *Behavior research methods*. 2012;44(4):1239-1243.
80. Pollatos O, Schandry R. Accuracy of heartbeat perception is reflected in the amplitude of the heartbeat-evoked brain potential. *Clinical Trial. Psychophysiology*. May 2004;41(3):476-82. doi:10.1111/1469-8986.2004.00170.x
81. Terhaar J, Viola FC, Bar KJ, Debener S. Heartbeat evoked potentials mirror altered body perception in depressed patients. *Clinical neurophysiology : official journal of the International Federation of Clinical Neurophysiology*. Oct 2012;123(10):1950-7. doi:10.1016/j.clinph.2012.02.086
82. Schandry R, Montoya P. Event-related brain potentials and the processing of cardiac activity. Research Support, Non-U.S. Gov't. *Biological psychology*. Jan 5 1996;42(1-2):75-85.
83. Salamone PC, Esteves S, Sinay VJ, et al. Altered neural signatures of interoception in multiple sclerosis. *Hum Brain Mapp*. 2018;39(12):4743-4754. doi:10.1002/hbm.24319

84. Garcia-Cordero I, Esteves S, Mikulan EP, et al. Attention, in and Out: Scalp-Level and Intracranial EEG Correlates of Interoception and Exteroception. *Frontiers in neuroscience*. 2017;11:411. doi:10.3389/fnins.2017.00411
85. Yoris A, Abrevaya S, Esteves S, et al. Multilevel convergence of interoceptive impairments in hypertension: New evidence of disrupted body-brain interactions. *Human brain mapping*. Apr 2018;39(4):1563-1581. doi:10.1002/hbm.23933
86. Dirlich G, Vogl L, Plaschke M, Strian F. Cardiac field effects on the EEG. *Electroencephalography and clinical neurophysiology*. Apr 1997;102(4):307-15.
87. Yoris A, Garcia AM, Traiber L, et al. The inner world of overactive monitoring: neural markers of interoception in obsessive-compulsive disorder. *Psychol Med*. 2017;47(11):1957-1970. doi:10.1017/S0033291717000368
88. Zich C, Debener S, Kranczioch C, Bleichner MG, Gutberlet I, De Vos M. Real-time EEG feedback during simultaneous EEG-fMRI identifies the cortical signature of motor imagery. *Neuroimage*. 2015;114:438-47. doi:10.1016/j.neuroimage.2015.04.020
89. Nichols TE, Das S, Eickhoff SB, et al. Best practices in data analysis and sharing in neuroimaging using MRI. *Nat Neurosci*. 2017;20(3):299-303. doi:10.1038/nrn.4500
90. Poldrack RA, Baker CI, Durnez J, et al. Scanning the horizon: towards transparent and reproducible neuroimaging research. *Nature reviews Neuroscience*. 2017;18(2):115-126. doi:10.1038/nrn.2016.167
91. Gonzalez CC, Salamone P, Rodríguez-Arriagada N, et al. Fatigue in multiple sclerosis is associated with multimodal interoceptive abnormalities. *Multiple Sclerosis Journal*. 2019:1352458519888881-1352458519888881.
92. Ashburner J, Friston KJ. Voxel-based morphometry--the methods. *Neuroimage*. 2000;11(6):805-21. doi:10.1006/nimg.2000.0582
93. Ashburner J. A fast diffeomorphic image registration algorithm. *Neuroimage*. 2007;38(1):95-113.
94. Burton EJ, McKeith IG, Burn DJ, Williams ED, O'Brien JT. Cerebral atrophy in Parkinson's disease with and without dementia: a comparison with Alzheimer's disease, dementia with Lewy bodies and controls. *Brain*. 2004;127(4):791-800.
95. Jack CR, Petersen RC, Xu YC, et al. Medial temporal atrophy on MRI in normal aging and very mild Alzheimer's disease. *Neurology*. 1997;49(3):786-794.
96. La Joie R, Perrotin A, Barré L, et al. Region-specific hierarchy between atrophy, hypometabolism, and  $\beta$ -amyloid (A $\beta$ ) load in Alzheimer's disease dementia. *J Neurosci*. 2012;32(46):16265-16273.

97. van Loenhoud AC, Wink AM, Groot C, et al. A neuroimaging approach to capture cognitive reserve: application to Alzheimer's disease. *Hum Brain Mapp*. 2017;38(9):4703-4715.
98. Chung J, Yoo K, Lee P, et al. Normalization of cortical thickness measurements across different T1 magnetic resonance imaging protocols by novel W-Score standardization. *Neuroimage*. 2017;159:224-235.
99. Ossenkoppelle R, Pijnenburg YA, Perry DC, et al. The behavioural/dysexecutive variant of Alzheimer's disease: clinical, neuroimaging and pathological features. *Brain*. 2015;138(9):2732-2749.
100. Zimmerman DW. Increasing the power of nonparametric tests by detecting and downweighting outliers. *The Journal of Experimental Education*. 1995;64(1):71-78.
101. Zamorano F, Billeke P, Kausel L, et al. Lateral prefrontal activity as a compensatory strategy for deficits of cortical processing in Attention Deficit Hyperactivity Disorder. *Sci Rep*. 2017;7(1):7181. doi:10.1038/s41598-017-07681-z
102. Billeke P, Armijo A, Castillo D, et al. Paradoxical Expectation: Oscillatory Brain Activity Reveals Social Interaction Impairment in Schizophrenia. *Biol Psychiatry*. 2015;78(6):421-431. doi:10.1016/j.biopsych.2015.02.012
103. Zamorano F, Billeke P, Hurtado J, et al. Temporal constraints of behavioral inhibition: relevance of inter-stimulus interval in a Go-Nogo task. *PLoS One*. 2014;9(1):e87232.
104. Shany-Ur T, Lin N, Rosen HJ, Sollberger M, Miller BL, Rankin KP. Self-awareness in neurodegenerative disease relies on neural structures mediating reward-driven attention. *Brain*. 2014;137(8):2368-2381.
105. Chiong W, Wood KA, Beagle AJ, et al. Neuroeconomic dissociation of semantic dementia and behavioural variant frontotemporal dementia. *Brain*. 2016;139(2):578-587.
106. Garcia-Cordero I, Sedeño L, Babino A, et al. Explicit and implicit monitoring in neurodegeneration and stroke. *Scientific reports*. 2019;9(1):1-10.
107. Langella S, Sadiq MU, Mucha PJ, Giovanello KS, Dayan E. Lower functional hippocampal redundancy in mild cognitive impairment. *Translational Psychiatry*. 2021;11(1):1-12.
108. Kumfor F, Ibañez A, Hutchings R, Hazelton JL, Hodges JR, Piguet O. Beyond the face: how context modulates emotion processing in frontotemporal dementia subtypes. *Brain*. 2018;141(4):1172-1185.
109. Kumfor F, Irish M, Hodges JR, Piguet O. Discrete neural correlates for the recognition of negative emotions: insights from frontotemporal dementia. *PLoS One*. 2013;8(6)

110. Crawford JR, Garthwaite PH, Porter S. Point and interval estimates of effect sizes for the case-controls design in neuropsychology: rationale, methods, implementations, and proposed reporting standards. *Cognitive neuropsychology*. 2010;27(3):245-260.
111. Voegler R, Peterburs J, Bellebaum C, Straube T. Modulation of feedback processing by social context in social anxiety disorder (SAD)—an event-related potentials (ERPs) study. *Scientific reports*. 2019;9(1):1-14.
112. Boudewyn MA, Luck SJ, Farrens JL, Kappenman ES. How many trials does it take to get a significant ERP effect? It depends. *Psychophysiology*. 2018;55(6):e13049.
113. Clayson PE, Baldwin SA, Larson MJ. How does noise affect amplitude and latency measurement of event-related potentials (ERPs)? A methodological critique and simulation study. *Psychophysiology*. 2013;50(2):174-186.
114. Poulsen C, Luu P, Davey C, Tucker DM. Dynamics of task sets: evidence from dense-array event-related potentials. *Cognitive brain research*. 2005;24(1):133-154.
115. Baker E, Veytsman E, Martin AM, Blacher J, Stavropoulos KK. Increased neural reward responsivity in adolescents with ASD after social skills intervention. *Brain Sciences*. 2020;10(6):402.
116. Depue BE, Ketz N, Mollison MV, Nyhus E, Banich MT, Curran T. ERPs and neural oscillations during volitional suppression of memory retrieval. *J Cogn Neurosci*. 2013;25(10):1624-1633.
117. Maris E, Oostenveld R. Nonparametric statistical testing of EEG- and MEG-data. *J Neurosci Methods*. 2007;164(1):177-90. doi:10.1016/j.jneumeth.2007.03.024
118. Bullmore ET, Suckling J, Overmeyer S, Rabe-Hesketh S, Taylor E, Brammer MJ. Global, voxel, and cluster tests, by theory and permutation, for a difference between two groups of structural MR images of the brain. *IEEE Trans Med Imaging*. 1999;18(1):32-42.
119. Chennu S, Noreika V, Gueorguiev D, et al. Expectation and Attention in Hierarchical Auditory Prediction. *J Neurosci*. 2013;33(27):11194-11205. doi:10.1523/JNEUROSCI.0114-13.2013
120. Manly B. *Randomization, bootstrap, and monte carlo methods in biology*. vol Third. Chapman & Hall; 2007.
121. Nichols TE. Multiple testing corrections, nonparametric methods, and random field theory. *Neuroimage*. 2012;62(2):811-815.
122. Sollberger M, Stanley CM, Wilson SM, et al. Neural basis of interpersonal traits in neurodegenerative diseases. *Neuropsychologia*. 2009;47(13):2812-2827.

123. Irish M, Addis DR, Hodges JR, Piguet O. Considering the role of semantic memory in episodic future thinking: evidence from semantic dementia. *Brain*. 2012;135(7):2178-2191.
124. Irish M, Piguet O, Hodges JR, Hornberger M. Common and unique gray matter correlates of episodic memory dysfunction in frontotemporal dementia and Alzheimer's disease. *Hum Brain Mapp*. 2014;35(4):1422-1435.
125. Santamaría-García H, Baez S, Reyes P, et al. A lesion model of envy and Schadenfreude: legal, deservingness and moral dimensions as revealed by neurodegeneration. *Brain*. 2017;140(12):3357-3377.
126. Garcia-Cordero I, Migeot J, Fittipaldi S, et al. Metacognition of emotion recognition across neurodegenerative diseases. *Cortex*. 2021;137:93-107.
127. Ibañez A, Fittipaldi S, Trujillo C, et al. Predicting and Characterizing Neurodegenerative Subtypes with Multimodal Neurocognitive Signatures of Social and Cognitive Processes. *Journal of Alzheimer's Disease*. 2021;(Preprint):1-22.
128. Bertoux M, Duclos H, Caillaud M, et al. When affect overlaps with concept: emotion recognition in semantic variant of primary progressive aphasia. *Brain*. 2020;143(12):3850-3864.
129. Fernández-Cabello S, Kronbichler M, Van Dijk KR, Goodman JA, Spreng RN, Schmitz TW. Basal forebrain volume reliably predicts the cortical spread of Alzheimer's degeneration. *Brain*. 2020;143(3):993-1009.
130. Han H, Glenn AL, Dawson KJ. Evaluating alternative correction methods for multiple comparison in functional neuroimaging research. *Brain sciences*. 2019;9(8):198.
131. Sankar A, Yttredahl AA, Fourcade EW, et al. Dissociable neural responses to monetary and social gain and loss in women with major depressive disorder. *Frontiers in behavioral neuroscience*. 2019;13:149.
132. Subramaniam K, Gill J, Slattery P, et al. Neural mechanisms of positive mood induced modulation of reality monitoring. *Frontiers in human neuroscience*. 2016;10:581.
133. Legaz A. Socially Reinforced Learning in Neurodegeneration - ANID/FONDECYT (1170010). [osf.io/9nw8j](https://osf.io/9nw8j)
134. Kumfor F, Hutchings R, Irish M, et al. Do I know you? Examining face and object memory in frontotemporal dementia. *Neuropsychologia*. 2015;71:101-111.
135. Ramanan S, Bertoux M, Flanagan E, et al. Longitudinal executive function and episodic memory profiles in behavioral-variant frontotemporal dementia and Alzheimer's disease. *J Int Neuropsychol Soc*. 2017;23(1):34-43.



136. Barnett JH, Blackwell AD, Sahakian BJ, Robbins TW. The paired associates learning (PAL) test: 30 years of CANTAB translational neuroscience from laboratory to bedside in dementia research. *Translational neuropsychopharmacology*. 2015;449-474.
137. Maass A, Berron D, Harrison TM, et al. Alzheimer's pathology targets distinct memory networks in the ageing brain. *Brain*. 2019;142(8):2492-2509.
138. Dermody N, Wong S, Ahmed R, Piguet O, Hodges JR, Irish M. Uncovering the neural bases of cognitive and affective empathy deficits in Alzheimer's disease and the behavioral-variant of frontotemporal dementia. *Journal of Alzheimer's Disease*. 2016;53(3):801-816.
139. Pfabigan DM, Gittenberger M, Lamm C. Social dimension and complexity differentially influence brain responses during feedback processing. *Social neuroscience*. 2019;14(1):26-40.
140. Shen Q, Zhu L, Meng L, et al. To reveal or not to reveal? Observation of social outcomes facilitates reward processing. *Frontiers in neuroscience*. 2020;14
141. Ibanez A, Melloni M, Huepe D, et al. What event-related potentials (ERPs) bring to social neuroscience? *Soc Neurosci*. 2012;7(6):632-49. doi:10.1080/17470919.2012.691078
142. Lockwood PL, Klein-Flügge M. Computational modelling of social cognition and behaviour—a reinforcement learning primer. *Social cognitive affective neuroscience*. 2020;16(8):761-771.
143. Gratwicke J, Jahanshahi M, Foltynie T. Parkinson's disease dementia: a neural networks perspective. *Brain*. 2015;138(6):1454-1476.
144. Bertoux M, Delavest M, de Souza LC, et al. Social cognition and emotional assessment differentiates frontotemporal dementia from depression. *J Neurol Neurosurg Psychiatry*. 2012;83(4):411-416.
145. Olsson A, Knapska E, Lindström B. The neural and computational systems of social learning. *Nature Reviews Neuroscience*. 2020;21(4):197-212.
146. Carter RM, Huettel SA. A nexus model of the temporal–parietal junction. *Trends in cognitive sciences*. 2013;17(7):328-336.
147. Rolls ET. Limbic systems for emotion and for memory, but no single limbic system. *Cortex*. 2015;62:119-157.
148. Rolls ET. The cingulate cortex and limbic systems for emotion, action, and memory. *Brain Structure and Function*. 2019;224(9):3001-3018.
149. Apps MA, Rushworth MF, Chang SW. The anterior cingulate gyrus and social cognition: tracking the motivation of others. *Neuron*. 2016;90(4):692-707.
150. Rudebeck PH, Rich EL. Orbitofrontal cortex. *Curr Biol*. 2018;28(18):R1083-R1088.

151. Spurny B, Seiger R, Moser P, et al. Hippocampal GABA levels correlate with retrieval performance in an associative learning paradigm. *Neuroimage*. 2020;204:116244.
152. Simon JR, Vaidya CJ, Howard Jr JH, Howard D. The effects of aging on the neural basis of implicit associative learning in a probabilistic triplets learning task. *J Cogn Neurosci*. 2012;24(2):451-463.
153. Burdakov D, Peleg-Raibstein D, Behavior. The hypothalamus as a primary coordinator of memory updating. *Physiol Behav*. 2020;223:112988.
154. Hinojosa J, Mercado F, Carretié L. N170 sensitivity to facial expression: A meta-analysis. *Neuroscience Biobehavioral Reviews*. 2015;55:498-509.
155. García-García I, Zeighami Y, Dagher A. Reward prediction errors in drug addiction and Parkinson's disease: from neurophysiology to neuroimaging. *Current neurology and neuroscience reports*. 2017;17(6):46.
156. Wikenheiser AM, Marrero-Garcia Y, Schoenbaum G. Suppression of ventral hippocampal output impairs integrated orbitofrontal encoding of task structure. *Neuron*. 2017;95(5):1197-1207. e3.
157. Ibáñez A. Insular networks and intercognition in the wild. *Cortex*. 2019;115:341.
158. Moretti L, Dragone D, Di Pellegrino G. Reward and social valuation deficits following ventromedial prefrontal damage. *J Cogn Neurosci*. 2009;21(1):128-140.
159. Hughes LE, Nestor PJ, Hodges JR, Rowe JB. Magnetoencephalography of frontotemporal dementia: spatiotemporally localized changes during semantic decisions. *Brain*. 2011;134(9):2513-2522.
160. Chan RC, Shum D, Touloupoulou T, Chen EY. Assessment of executive functions: Review of instruments and identification of critical issues. *Archives of clinical neuropsychology*. 2008;23(2):201-216.
161. Luria R, Sessa P, Gotler A, Jolicœur P, Dell'Acqua R. Visual short-term memory capacity for simple and complex objects. *J Cogn Neurosci*. 2010;22(3):496-512.
162. Tzourio-Mazoyer N, Landeau B, Papathanassiou D, et al. Automated anatomical labeling of activations in SPM using a macroscopic anatomical parcellation of the MNI MRI single-subject brain. *Neuroimage*. 2002;15(1):273-89. doi:10.1006/nimg.2001.0978
163. Lenhard W, Lenhard A. Calculation of effect sizes. Dettelbach, Germany; 2016.

## Figure legends

**Figure 1 SRL task and behavioral results. (A) SRL task design.** Participants judged whether three-digit numbers presented repeatedly on a computer screen belonged to either category “A” or “B”. Visual feedback immediately followed each number-category judgement (smiling face for correct responses or angry face for incorrect responses in the SRL condition; green circle for correct responses or red circle for incorrect responses in the NSRL condition). High-density EEG recordings were obtained during the task. **(B) Behavioral results in HCs.** *Left:* repeated measures ANOVA of accuracy across cycles and feedback conditions. *Right:* One-way ANOVA between feedback conditions for the learning index (Spearman's rank correlation coefficient values for the accuracy score by cycle). The mean difference (effect size) of the between-conditions comparison in HCs (NSRL minus SRL) is reported. **(C) Behavioral results: between-group comparisons.** Learning index for comparisons of behavioral performance between groups, for SRL and NSRL conditions. The between-groups mean difference (effect size) between HCs and each neurodegenerative group is reported below each result. Behavioral results were replicated when controlling for sex and valence recognition (see **Supplementary Material 3.5** and **Supplementary Material 3.6** for details). The asterisk (\*) indicates significant differences with an alpha of  $P < 0.05$ . AD: Alzheimer's disease, bvFTD: behavioral variant of fronto-temporal dementia, HCs: healthy controls, NSRL: non-socially reinforced learning, PD: Parkinson's disease, SRL: Socially reinforced learning.

**Figure 2 Spatiotemporal cluster results for SRL. (A) SRL vs NSRL conditions for each group.** Pink and grey solid curves show the average values of the maximum cluster, while pink and grey dashed curves show the average values of a reference electrode yielding maximum difference by univariate  $t$ -test. **(B) Initial set vs final set comparison in the SRL condition.** Dark pink and light pink solid curves show the average values of the maximum cluster, while dark pink and light pink dashed curves show the average values of a reference electrode yielding maximum difference by univariate  $t$ -test. Shaded bars around solid curves indicate SEM. Scalp plots show, for significant clusters, the  $t$ -values obtained at time marked by the black vertical dashed line for the electrodes belonging to the cluster (small white dots) and, for the non-significant clusters, the  $t$ -values obtained at time marked by the black vertical dashed line for all the electrodes. Black vertical dashed line shows the time when the maximum

difference was obtained for the reference electrode (large white black-contoured dot). Black horizontal rectangle indicates time interval where the cluster results are statistically significant. AD: Alzheimer's disease, bvFTD: behavioral variant of fronto-temporal dementia, HCs: healthy controls, NSRL: non-socially reinforced learning, PD: Parkinson's disease, SRL: socially reinforced learning.

**Figure 3 Associations between GM volume and SRL/NSRL indexes.** These analyses were conducted to identify regions, in all groups together and in separate tandems (bvFTD-HCs, PD-HCs, and AD-HCs) associated with SRL and NSRL performance (SnPM, 5000 permutations, cluster-wise inference  $P\text{-FWE} < 0.05$ ). Results are presented on MNI space using the AAL atlas,<sup>162</sup> in the neurological convention. No significant structural associations were found in the PD group. R: right; L: left. AD: Alzheimer's disease, ALL: all groups, bvFTD: behavioral variant frontotemporal dementia; NSRL: non-socially reinforced learning, PD: Parkinson's disease, SRL: socially reinforced learning.

**Figure 4 Anatomical conjunction of SRL and NSRL conditions.** Whole-brain conjunction analyses were conducted in order to assess the shared and distinct neural correlates of SRL and NSRL conditions. Results are presented on MNI space using the AAL atlas,<sup>162</sup> in neurological convention. Blue represents significant clusters of SRL. Green represents significant clusters of NSRL. Red represents overlapping clusters between SRL and NSRL conditions (right parahippocampus [peak MNI coordinate:  $x = 22.5$ ;  $y = -22.5$ ;  $z = -15$ ;  $k = 292$ ], and right hypothalamus [peak MNI coordinate:  $x = 15$ ;  $y = -4.5$ ;  $z = -10.5$ ;  $k = 224$ ]). NSRL: non-socially reinforced learning, SRL: socially reinforced learning.

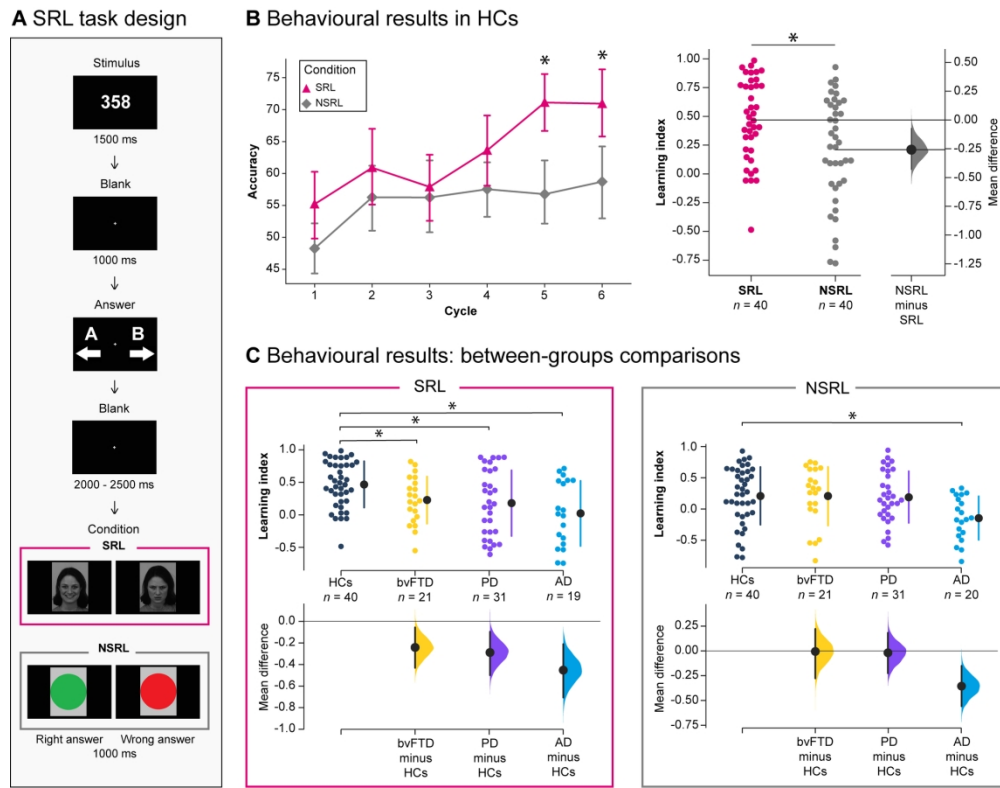


Figure 1

181x141mm (300 x 300 DPI)

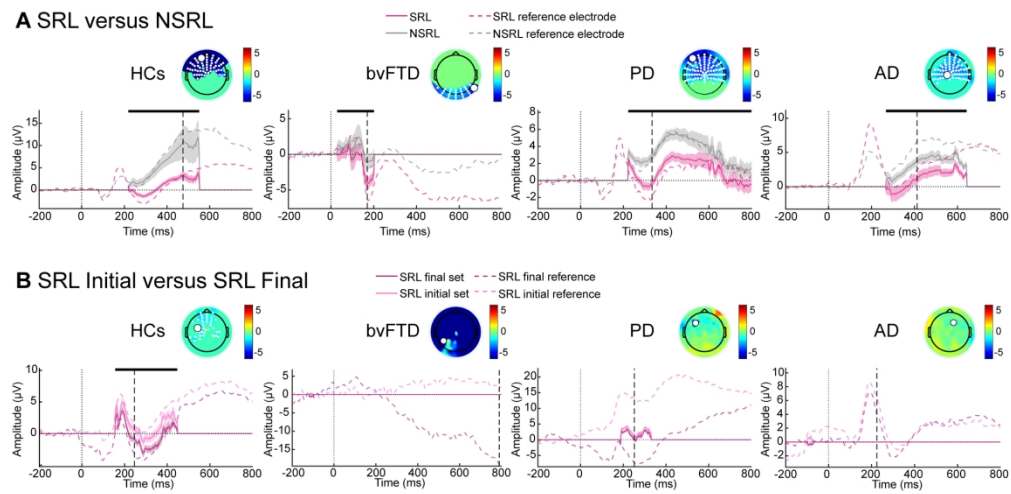


Figure 2

184x89mm (300 x 300 DPI)

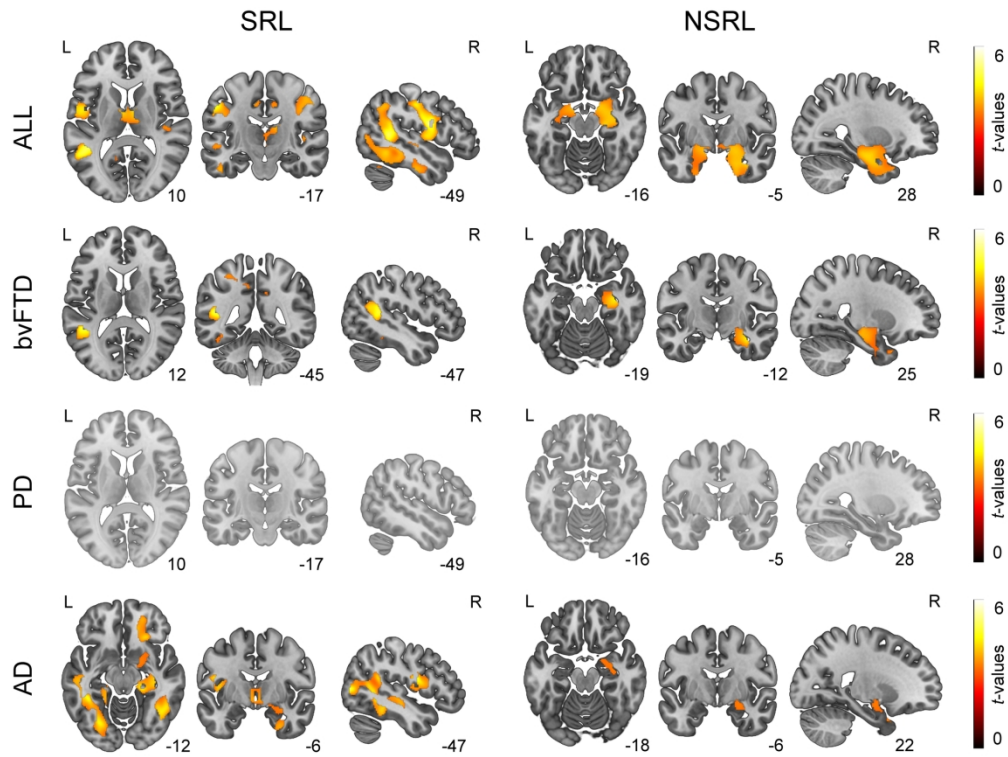


Figure 3

182x136mm (300 x 300 DPI)

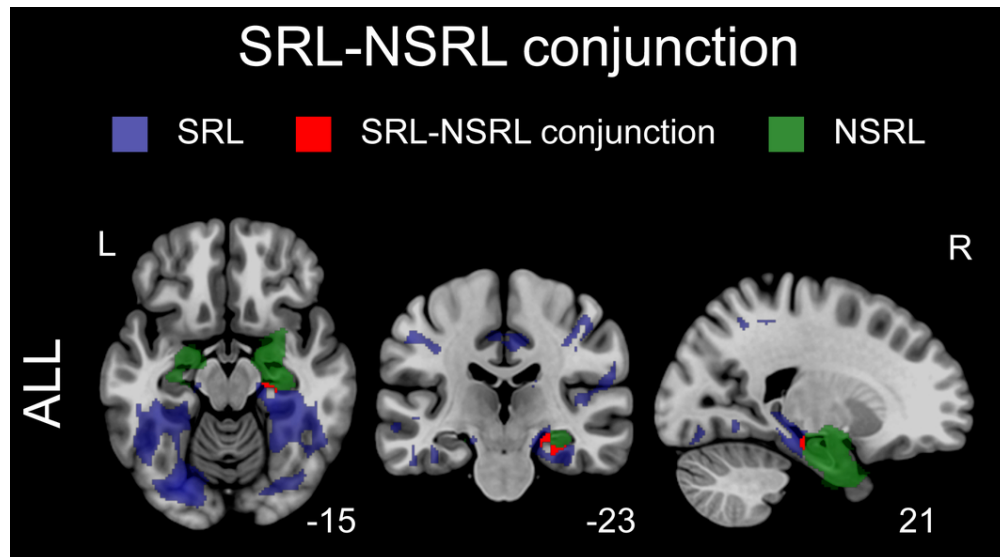




Table 1 Previous studies that assessed social learning and feedback-based learning in behavioral variant frontotemporal dementia, Alzheimer’s disease, and/or Parkinson’s disease

Authors / Journal	Groups: <i>n</i>	Tasks	Behavioral performance	¿Social information improves learning?	EEG, brain structural and/or functional associations
Keri, (2014). <i>Cortex</i> . <sup>33</sup>	Early-stage bvFTD: 16, elderly, early-stage AD: 20, HCs: 20	Paired-associate learning task: real-life game (real persons) ( <b>social</b> ) vs. computer games (boxes and neutral faces) ( <b>non-social</b> )	Real-life game: HCs = AD > bvFTD Computer games: HCs = bvFTD > AD	Yes, only real-life interactions improved associative learning in early-stage AD	NA
Wong <i>et al.</i> , (2017). <i>Neuropsychologia</i> . <sup>36</sup>	bvFTD: 20, AD: 14, HCs: 20	Trust game task: steal/share associated to face ( <b>social</b> ) vs. lottery ( <b>non-social</b> )	Social learning accuracy: HCs > bvFTD = AD	No, reduced capacity to learn socially relevant information in both bvFTD and AD	GM atrophy (VBM) correlations for <b>bvFTD</b> (Lateral occipital cortex, superior temporal gyrus, middle temporal gyrus, frontal pole, orbitofrontal cortex, putamen, middle frontal gyrus) and for <b>AD</b> (Superior temporal gyrus, cerebellum, parahippocampal gyrus, hippocampus, lateral occipital cortex)
Duff <i>et al.</i> , (2013). <i>The Journal of Comparative Neurology</i> . <sup>34</sup>	Early-stage AD: 5, HCs: 10	Collaborative referencing task (real-life interactive learning task) ( <b>social</b> ) vs. paired-associate learning control task ( <b>non-social</b> )	Collaborative referencing task: HCs = AD Paired-associate learning control task: HCs > AD	Yes, real-life interactions with a familiar person improved associative learning in early-stage AD	NA
Schmitt-Eliassen <i>et al.</i> , (2007). <i>Brain Research</i> . <sup>42</sup>	PD: 31, elderly HCs: 30	Feedback-based learning task vs. observational learning task ( <b>only non-social</b> )	Feedback-based task: HCs = PD (but no learning effect under feedback-based task compared to observational task in neither group)	NA	NA
Meissner <i>et al.</i> , (2016). <i>Behavioural Brain Research</i> . <sup>41</sup>	PD: 18, HCs: 18	Feedback-based learning task ( <b>only non-social</b> )	Feedback-based task: HCs > PD	NA	NA
Shohamy <i>et al.</i> , (2004). <i>Brain</i> . <sup>43</sup>	PD: 13, HCs: 13	Feedback-based learning task vs. observational learning task ( <b>only non-social</b> )	Feedback-based task: HCs > PD Observational task: HCs = PD	NA	NA

AD: Alzheimer’s disease, bvFTD: behavioral variant of fronto-temporal dementia, HCs: healthy controls, GM: grey matter; PD: Parkinson’s disease, VBM: Voxel-based morphometry.

Downloaded from https://academic.oup.com/brain/advance-article/doi/10.1093/brain/awab345/6371182 by guest on 27 September 2021

Table 2 Samples' demographic and neuropsychological data

	HCS ( <i>n</i> = 40)	bvFTD ( <i>n</i> = 21)	PD ( <i>n</i> = 31)	AD ( <i>n</i> = 20)	Stats	<i>Post hoc</i> comparisons
<b>Demographics</b>						
Sex <sup>†</sup> (M:F)	18:22	16:05	18:13	9:11	$\chi^2 = 6.32$ $P = 0.09$	HCS-bvFTD: $P = 0.02^*$ HCS-PD: $P = 0.27$ HCS-AD: $P = 1$
Age <sup>†</sup>	68.92 (8.66)	66.67 (11.52)	70.48 (9.10)	73.00 (6.01)	$F = 1.86$ $P = 0.13$ $\eta p^2 = 0.04$	HCS-bvFTD: $P = 0.35$ HCS-PD: $P = 0.47$ HCS-AD: $P = 0.10$
Education	13.90 (3.67)	14.43 (5.03)	12.29 (4.31)	12.30 (4.00)	$F = 1.76$ $P = 0.15$ $\eta p^2 = 0.04$	HCS-bvFTD: $P = 0.64$ HCS-PD: $P = 0.11$ HCS-AD: $P = 0.16$
Handedness (R:L)	38:2	20:1	29:2	19:1	–	–
<b>Cognitive assessment</b>						
MoCA <sup>†</sup>	25.59 (2.57)	21.00 (5.51)	21.93 (4.31)	16.11 (4.46)	$F = 24.14$ $P < 0.001^*$ $\eta p^2 = 0.40$	HCS-bvFTD: $P < 0.001^*$ HCS-PD: $P < 0.001^*$ HCS-AD: $P < 0.001^*$
IFS <sup>†</sup>	22.09 (3.79)	18.62 (6.30)	19.88 (4.12)	14.97 (4.38)	$F = 11.30$ $P < 0.001^*$ $\eta p^2 = 0.24$	HCS-bvFTD: $P = 0.006^*$ HCS-PD: $P = 0.05$ HCS-AD: $P < 0.001^*$

Results are presented as mean (SD). Lower executive function scores (IFS) in AD are triggered by advanced age and lower general cognitive state.<sup>162</sup> Demographic and cognitive data were assessed through ANOVAs and *post hoc* pairwise comparisons –except for sex, which was analyzed via Pearson's chi-squared ( $\chi^2$ ) test. Effects sizes were calculated through partial eta ( $\eta p^2$ ). AD: Alzheimer's disease, bvFTD: behavioral variant of fronto-temporal dementia, HCS: healthy controls, IFS: INECO Frontal Screening,<sup>163</sup> MoCA: Montreal Cognitive Assessment,<sup>164</sup> PD: Parkinson's disease.

\*Significant differences with an alpha level of  $P < 0.05$ .

<sup>†</sup>Variables with significant differences ( $P < 0.05$ ) between neurodegenerative groups, precluding comparisons between them in our target measures.

Table 3 Feedback valence ratings

Feedback Accuracy	HCs ( <i>n</i> = 40)	bvFTD ( <i>n</i> = 21)	PD ( <i>n</i> = 31)	AD ( <i>n</i> = 20)
Total	0.94 (0.24)	0.88 (0.33)	0.80 (0.4)	0.81 (0.39)
Social	0.90 (0.30)	0.92 (0.27)	0.81 (0.40)	0.85 (0.36)
Non-social	0.98 (0.16)	0.82 (0.38)	0.79 (0.41)	0.78 (0.42)
Social positive	0.90 (0.30)	1 (0)	0.81 (0.40)	0.85 (0.37)
Social negative	0.90 (0.30)	0.85 (0.37)	0.81 (0.40)	0.85 (0.37)
Non-social positive	0.98 (0.16)	0.90 (0.31)	0.84 (0.37)	0.85 (0.37)
Non-social negative	0.98 (0.16)	0.75 (0.44)	0.74 (0.44)	0.70 (0.47)

Results are presented as mean (*SD*). To assess feedback valence recognition among groups, participants were explicitly asked about the valence (positive, negative) of each feedback type [Social (smiling face, angry face); Non-social (green circle, red circle)] at the end of the experiment. All groups presented adequate valence recognition (with no significant differences; for details see **Supplementary Material 2.1**). AD: Alzheimer's disease, bvFTD: behavioral variant of fronto-temporal dementia, HCs: healthy controls, PD: Parkinson's disease.

Table 4 Statistical comparison between groups (HCs, bvFTD, PD and AD) and conditions (SRL and NSRL) in the learning index

Kruskal-Wallis test							
Condition	HCs	bvFTD	PD	AD	Statistical results		
					<i>H</i>	<i>P</i>	$\eta^2[H]$
SRL	0.46 (0.35)	0.22 (0.35)	0.17 (0.49)	0.007 (0.48)	13.54	0.003*	0.097
NSRL	0.21 (0.45)	0.20 (0.45)	0.19 (0.40)	-0.14 (0.33)	10.89	0.01*	0.073
Mann-Whitney U							
	HCs	Neurodegenerative's samples		Statistical results			
				<i>U</i>	<i>P</i>	Cohen's <i>d</i>	
SRL	0.46 (0.35)	bvFTD: 0.22 (0.35)		577	0.017*	0.641	
		PD: 0.17 (0.49)		830.5	0.014*	0.605	
		AD: 0.007 (0.48)		186	0.001*	0.961	
NSRL	0.21 (0.45)	bvFTD: 0.20 (0.45)		419.5	0.997	0.002	
		PD: 0.19 (0.40)		655.5	0.684	0.098	
		AD: -0.14 (0.33)		210.5	0.003*	0.831	

Results are presented as mean (*SD*). The asterisk (\*) indicates significant differences with an alpha level of  $P < 0.05$ . Learning Index (Spearman correlation's Rho slope of cycles and accuracy score) were assessed through nonparametric Kruskal-Wallis tests (with two-tail Mann-Whitney-U tests for post hoc comparisons). Effect size for the Kruskal-Wallis test was calculated as the eta-squared based on the *H*-statistic:  $(H - k + 1)/(n - k)$ , *k* being the number of groups, and for the Mann-Whitney U the Cohen's *d* value was obtained.<sup>163</sup> AD: Alzheimer's disease, bvFTD: behavioral variant of fronto-temporal dementia, HCs: healthy controls, PD: Parkinson's disease.